Mechanism for Transduction of the Ligand-Binding Signal in Heme-Based Gas Sensory Proteins Revealed by Resonance Raman Spectroscopy

TAKESHI UCHIDA AND TEIZO KITAGAWA*
Okazaki Institute for Integrative Bioscience, National Institutes of Natural Sciences, Myodaiji, Okazaki, Aichi 444-8787, Japan

Received November 30, 2004

ABSTRACT
Gene analysis has revealed a variety of new heme-containing gas sensory proteins in organisms ranging from bacteria to mammals. These proteins are composed of sensor, communication, and functional domains. The sensor domain contains a heme that binds effector molecules such as NO, O_2, or CO. Ligand binding by the sensor domain modulates the physiological role of the protein, such as DNA binding in the case of transcriptional factors or the catalytic reaction rate in the case of enzymes. This Account summarizes resonance Raman (RR) studies, including static and time-resolved measurements, which have enabled elucidation of the mechanisms by which binding of specific target molecule by the sensor domain is transduced to alteration of the functional domain. These studies have shown that signals can be conveyed from the heme to the functional domain via three different pathways: (i) a distal pathway, (ii) a proximal pathway, and (iii) a heme peripheral pathway.

Introduction

Heme proteins are one of the most versatile groups of proteins in living cells. Their functions range from electron transfer (e.g., cytochromes)[1,2] to oxygen transport (e.g., hemoglobin [Hb]), oxygen storage (e.g., myoglobin [Mb]),[3] and catalysis (e.g., P450 and cytochrome *c* peroxidase).[4,5] In recent years, the ability of heme proteins to sense and be regulated by gaseous diatomics, such as NO, O_2, and CO, has attracted considerable attention.[6−8] The heme-based gas sensor proteins discovered so far are listed in Table 1. All of these are homo- or heterodimers, and their activities are controlled by allosteric effects. In this regard, studies of the higher order structure of Hb and its change upon ligand binding provide some basic information about the structural mechanism of the allosteric effects.[9,10]

Soluble guanylate cyclase (sGC), which is expressed in the cytoplasm of almost all mammalian cells, is the only known NO sensor protein.[11] The protein isolated from bovine lung is a heterodimer composed of an α (M_r = 74 000) subunit and a β (M_r = 69 000) subunit that catalyzes the conversion of GTP to cGMP. His105 in the N-terminal region of the β subunit coordinates heme to which the signaling molecule, NO, binds,[12,13] while the catalytic site is located in the C-terminal region. When isolated, this protein contains an Fe^{II} heme that hardly binds O_2. It has been proposed that NO binding to sGC induces the cleavage of the Fe−His bond, which triggers conformational changes, increasing the cyclase activity by up to 200-fold, whereas binding of CO yields a six-coordinate (6c) heme that only marginally increases the activity (5-fold). Schematic model of sGC activation induced by NO binding is illustrated in Figure 1.

FixL and direct oxygen sensor (DOS), which have autophosphorylation and phosphodiesterase activities, respectively, are O_2 sensor heme proteins belonging to the PAS superfamily.[14,15] Although the functional properties of *Escherichia coli* DOS (*Ec* DOS) differ from those of FixL, they share a similar ligand-sensing mechanism. Both enzymes are active in the deoxy form but inactive in the O_2-bound form. Also, *Ec* DOS is inactive in the oxidized form. The X-ray crystal structure of FixL shows that O_2 binding to heme induces the rearrangement of the hydrogen-bonding network around the heme propionate groups, leading to the depression of kinase activity.[16] In the case of *Ec* Dos, Met95, which is an endogenous axial ligand of reduced heme, is replaced by O_2 in the O_2-bound form or by H_2O in the oxidized form, perturbing the hydrogen-bonding network, which involves Arg97, a heme propionate group, and water molecules.[17,18] This disruption of the hydrogen-bonding network results in decreased phosphodiesterase activity.

CooA, which belongs to the CRP family, and neuronal PAS domain protein 2 (NPAS2) are CO sensor proteins that function as transcriptional factors.[19] In CooA, CO binds to the ferrous 6c-LS heme by displacing an endogenous protein ligand, and this change of heme coordination induces binding of the functional domain to DNA and results in expression of the *coo* genes.[19] Cystathionine-β-synthase, which catalyzes the condensation of serine and homocysteine to give cystathionine, contains a heme with His and Cys as heme ligands as CooA does. Because this enzyme is expressed in only the brain and its enzymatic activity is inhibited by CO binding to heme, cystathionine-

Takeshi Uchida was born in Aomori Prefecture, Japan, in 1969. He received his B.Eng. (1993), M.Eng. (1995), and Ph.D. (1998) degrees from Kyoto University under the supervision of Prof. Isao Morishima. After undertaking postdoctoral work at the Institute for Molecular Science and at Albert Einstein College of Medicine, where he worked with Prof. Mark R. Chance, he joined the Institute for Molecular Science as a research associate of the research group of Prof. Teizo Kitagawa in 2001. His current research interests include the bioinorganic chemistry of heme-containing enzyme and sensor proteins.

Teizo Kitagawa was born in Kyoto, Japan, in 1940. He graduated from the engineering department of Osaka University in 1963 and received his M.Sci. and Ph.D. degrees in 1965 and 1969, respectively, from Osaka University, under the supervision of Prof. Tatsuo Miyazawa. He became a research associate of the Institute for Protein Research, Osaka University, in 1966, an associate professor of the Medical School of Osaka University in 1980, and a full professor of the Institute for Molecular Science in 1983. During the period in which he worked as a research associate, he studied the vibrational spectra of polymer crystals and related solid-state properties, including neutron inelastic scattering. In addition, he also studied liquid dynamics using ATR spectroscopy while working as a postdoctoral fellow for Prof. Bryce L. Crawford of the University of Minnesota. Since returning from the U.S.A., he has studied dynamic structure−function relationships of proteins using vibrational spectroscopy.

* To whom correspondence should be addressed. Telephone: 81-564-59-5225. Fax: 81-564-59-5229. E-mail: teizo@ims.ac.jp.

10.1021/ar030267d CCC: $30.25
Published on Web 06/24/2005

Table 1. Heme-Based Gas Sensor Proteins

effector	protein	function	source
NO	sGC[a]	conversion of GTP to cGMP	mammalian brain, lung, etc.
O_2	FixL	kinase	*Rhizobium meliloti*
			Bradyrhizobium japonicum
O_2	DOS	phosphodiesterase	*Escherichia coli*
O_2	PDEA1	phosphodiesterase	*Acetobacter xylinum*
O_2	HemAT	signal transducer for aerotaxis	*Bacillus subtilis*
			Halobacterium salinarum
CO	CooA	transcriptional activator	*Rhodospirillum rubrum*
CO	NPAS2	transcriptional factor	mammalian brain

[a] Abbreviations: sGC, soluble guanylate cyclase; DOS, direct oxygen sensor; PDEA1, phosphodiesterase protein A1; HemAT, heme-based aerotaxis transducer; NPAS2, neuronal PAS domain protein 2.

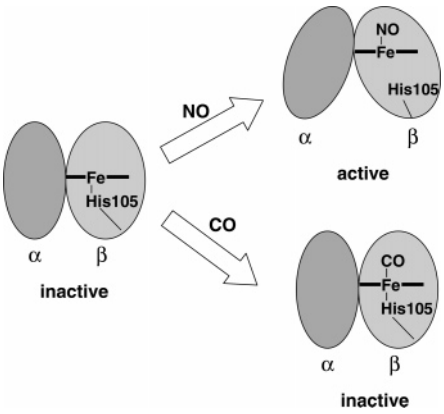

FIGURE 1. Schematic model of NO-induced activation of sGC. Heme is coordinated to His105 of the β subunit. When NO binds to heme, the bond between heme and His105 is cleaved, which induces conformational change of the protein and increases the enzyme activity. However, the heme−His105 bond is not cleaved by CO binding, which minimally affects the enzymatic activity.

β-synthase could be a CO sensor protein.[20] However, it is unclear at this moment whether this enzyme works as a gaseous sensor protein under physiological condition. Elucidation of the allosteric mechanisms in these proteins would have a great impact on protein chemistry. Accordingly, in this Account, we discuss the results of resonance Raman (RR) spectroscopic studies that have explored the mechanism by which the individual heme domains detect the binding of a specific diatomic molecule.

Overview of the RR Spectra of Sensor Hemoproteins

RR spectroscopy is a particularly useful technique for the structural characterization of heme and its immediate environment in proteins.[21] It is well-established that the high-frequency region of the Raman spectra is composed of porphyrin in-plane modes that are sensitive to the oxidation, spin, and coordination states of the heme iron.[21,22] The frequencies of the ν_2, ν_3, and ν_4 bands of known sensor hemoproteins for the Fe^{III}, Fe^{II}, and Fe^{II}-CO forms are compared in Table 2. For example, the ferric heme in the 5c-HS, 6c-HS, and 6c-LS states shows ν_3 bands (polarized) at 1490−1500, 1475−1485, and 1500−1510 cm^{-1}, respectively.[21]

The marker bands indicate that FixL and sGC have a 5c-HS heme, whereas CooA, NPAS2, and *Ec* DOS have a 6c-LS heme in both the ferric and ferrous states. Hb, which transports oxygen from the lung to internal tissues in mammals, has a ferrous 5c heme, the sixth coordination site of which is left open for ligand binding.[3] Other heme enzymes, such as cytochrome P450, catalase, and horseradish peroxide, also have a 5c heme in a substrate- or oxidant-bound form.[23] On the other hand, a 6c heme is observed in cytochromes *b* and *c*, which work as electron-transfer proteins and are generally unreactive toward gaseous ligands. Although the sensor hemoproteins must readily bind a specific ligand in response to changes in the ligand concentration, some of their hemes have no vacancy for exogenous ligand as those in cytochromes. Therefore, when an exogenous ligand binds to the 6c heme, it must replace one of the intrinsic ligands, which seems to be energetically disadvantageous. However, some sensory hemoproteins utilize the ligand replacement performed upon binding of an exogenous ligand to transduce the signal to the functional domain as discussed below.

Activation via the Distal Pathway

CooA, from the purple non-sulfur photosynthetic bacterium, *Rhodospirillum rubrum,* was the CO sensor protein reported first.[24] The ferrous CooA, which is inactive as a transcriptional factor, has a 6c heme with His77 and Pro2 as axial ligands.[25] It is very unique that His77 and Pro2 belong to different subunits in the dimer in addition to coordination of Pro. Binding of CO to the ferrous 6c heme converts CooA to an active form, in which Pro2 but not His77 is displaced by CO.[26,27] When Pro2 is displaced, it moves away from the heme pocket and interacts only weakly with the bound CO, as suggested by the behavior of the frequency of the Fe−CO stretching (ν_{Fe-CO}) mode as discussed next. Values for the Fe−CO mode of various sensory proteins are compared in Table 3.

Extensive studies using Mb mutants indicate that the frequency of ν_{Fe-CO} is a good indicator of the electrostatic fields around the bound ligand in the heme pocket.[28−30] When positively charged groups are predominant near the bound CO, the $Fe{=}C{=}O^{\delta-}\cdots X^{+}$ structure is stabilized (Figure 2A), which causes the frequency of ν_{Fe-CO} to increase and that of ν_{C-O} to decrease. In contrast, when negatively charged groups are predominant, the $Fe{-}C{\equiv}O^{\delta+}\cdots X^{-}$ structure is stabilized (Figure 2C), which causes the frequency of ν_{Fe-CO} to decrease and that of ν_{C-O} to increase. For Mb, in which a proton on the N_ϵ atom of

Table 2. Resonance Raman Characteristics of Sensor Hemoproteins

	effector	ν_2	ν_3	ν_4	coordination	references
Fe^{III}						
sGC	NO	1573	1495	1370	His	70
CooA	CO	1585	1504	1375	Cys/Pro	34
NPAS2 (PAS-A)	CO	1581, 1550	1504, 1490, 1471	1373	Cys/His	37
Ec DOS	O_2	1577	1505	1372	His/H_2O	56
FixL	O_2	1562	1493	1372	His	38, 71
Fe^{II}						
sGC	NO	1584	1468	1360	His	46
CooA	CO	1579	1491	1359	His/Pro	33, 34
NPAS2 (PAS-A)	CO	1557, 1584	1471, 1493	1360	His/His	37
Ec DOS	O_2	1580	1493	1361	His/Met	56
FixL	O_2	1558	1470	1355	His	72
HemAT	O_2	1558	1469	1352	His	68
$Fe^{II}CO$						
sGC	NO	1584	1499	1370	His/CO	46
CooA	CO	1580	1491	1371	His/CO	33, 34
NPAS2 (PAS-A)	CO	1583, 1556	1497, 1468	1372	His/CO	37
Ec DOS	O_2	1581	1496	1370	His/CO	56
FixL	O_2	NR	NR	1371	His/CO	71
HemAT	O_2	1578	1495	1368	His/CO	68

Table 3. Frequencies (cm^{-1}) of Iron−Ligand and Ligand Internal Stretching Modes of Sensor Hemoproteins

proteins	effector	ν_{Fe-His}	ν_{Fe-CO}	ν_{C-O}	ν_{Fe-O_2}	ν_{Fe-NO}	ν_{N-O}	references
sGC[a]	NO	204	472	1987	NR[b]	525	1677	47, 63
sGC[c]	NO	NR[b]	497	1959	NR[b]	520	NR[b]	46, 70
CooA	CO	211[d]	487	1969	NR[b]	NR[b]	NR[b]	33
CooA	CO	NR[b]	487	1983	NR[b]	523	1672	34
PAS-A	CO	220[d]	496	1962	NR[b]	NR[b]	NR[b]	37
Ec DOS	O_2	214[d]	486	1973	561	563	1632, 1576	56
FixL	O_2	209	498	1962	571	525	1676	38, 73
HemAT	O_2	225	494	1964	560	NR[b]	NR[b]	68

[a] Heme retained during isolation and purification procedures. [b] NR = not reported. [c] Heme reconstituted after isolation and purification procedures. [d] Observed only immediately after photolysis of the iron-bound CO.

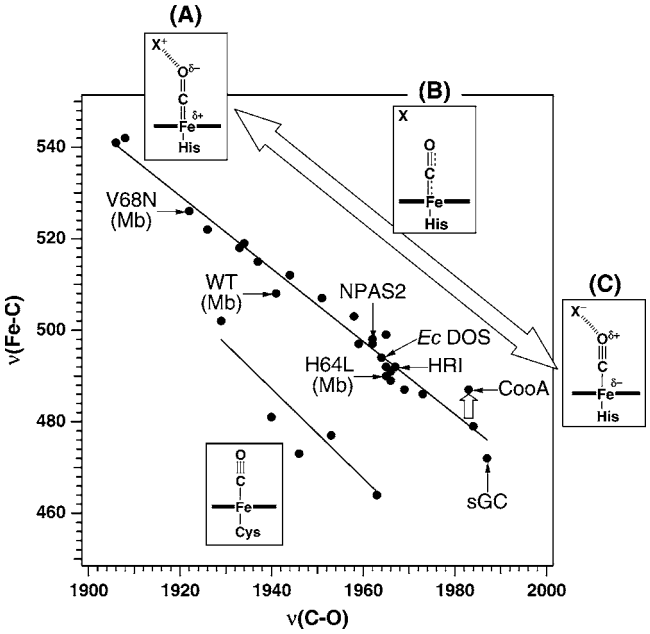

FIGURE 2. Correlation plot between ν_{Fe-CO} and ν_{C-O} of various hemoproteins. Schematic structures are illustrated in the insets.

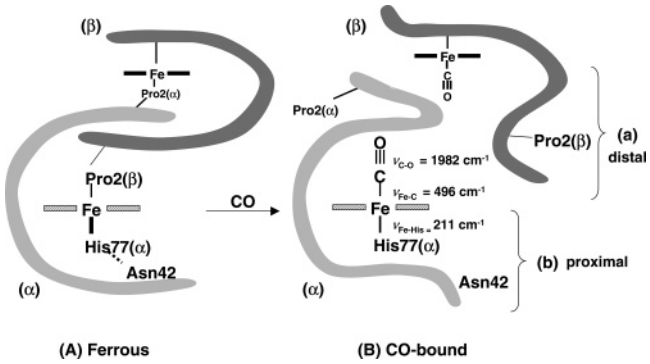

FIGURE 3. Schematic illustration of heme environmental structures of ferrous (A) and CO-bound CooA (B). a and b represent the distal and proximal pathways, respectively.

the so-called distal His (His64) is present near CO, ν_{Fe-CO} is observed at 508 cm^{-1} (Figure 2, WT),[29,31] whereas replacement of the distal His with Leu (H64L) decreases the ν_{Fe-CO} frequency to 490 cm^{-1}.[31] In contrast, addition of a positive charge by replacing Val at position 68 with Asn (V68N) increases the ν_{Fe-CO} frequency to 527 cm^{-1}.[32]

The ν_{Fe-CO} frequency of CO-bound CooA is observed at 487 cm^{-1},[33,34] which is similar to that observed for the H64L Mb mutant.[31] This suggests that the polarity of the distal side in CooA is comparable to that in the H64L Mb mutant (Figure 2B). If Pro2, which appears to have a negative charge based on the frequency of ν_{11},[35] interacts with bound CO, the ν_{Fe-CO} frequency of CooA would be significantly lower than that observed for the Mb H64L mutant. These results imply that Pro2 is not located near the iron-bound CO but moves out of the heme pocket when it is displaced by CO. This leads us to assume that this replacement of the heme ligand upon CO binding causes a large conformational change, allowing its binding to DNA at a distant region. Part a of Figure 3 shows a

schematic representation of the conformational change in CooA upon CO binding.

NPAS2, which is the second heme-based CO sensor protein discovered,[36] acts as a CO-dependent transcriptional factor for *clock* genes. In the absence of CO, it forms a heterodimer with BMAL1 and specifically binds to the E-box elements, whereas in the presence of CO, it dissociates from BMAL1 and DNA. Despite a lack of sequence homology with CooA, NPAS2 seems to have a mechanism of activation similar to that of CooA.[37] The reduced heme of the PAS-A domain of NPAS2 has 6c-LS heme with bis-histidine coordination. CO binds to the 6c heme of the PAS-A domain of NPAS2, which gives rise to the ν_{Fe-CO} band at 496 cm^{-1} (Table 3). This frequency also suggests that the replaced His does not interact with iron-bound CO (Figure 2). Thus, the movement of the coordinated residue outward from the heme pocket would cause a conformational change in the DNA-binding form, as observed for CooA. Accordingly, CooA and NPAS2 seem to utilize a common mechanism involving the distal pathway for transducing the ligand-binding signal. Such signal transduction mechanism via the distal side was also proposed in the O_2-sensing mechanism of FixL.[38] Furthermore, the allosteric mechanism controlled by distal interactions was found in Hb from *Mycobacterium tuberculosis*.[39] In this protein, O_2 binding to heme causes little structural arrangement on the proximal site but induces modulation of the hydrogen-bonding network including distal histidine, which leads to the allosteric structural transition.

Activation via the Proximal Pathway

Spiro and co-workers have proposed an alternative activation mechanism for transduction of the ligand-binding signal by CooA.[35] This mechanism assumes that modulation of bond strength between the heme iron and proximal His initiates the conformational change. The ν_{C-O} frequency of CooA observed at 1982 cm^{-1} [34,35] is somewhat higher than that predicted from the frequency of 487 cm^{-1} for ν_{Fe-CO} by the linear correlation line of neutral His-coordinated heme proteins shown in Figure 2. This was ascribed to a weak Fe−His bond because diminished σ bonding from the proximal ligand was deduced to cause a decrease in π back-donation from Fe to CO.[35] This idea is supported by the low Fe−His stretching mode (ν_{Fe-His}) at 211 cm^{-1} observed immediately after CO photolysis of CooA.[26] Contrary to the CO-bound form, the strength of the Fe−His bond of ferrous CooA was estimated to be as strong as that of Mb based on the ν_{Fe-His} frequency of the mutant CooA, which has a 5c heme in the ferrous state.[35] Indeed, the ν_{Fe-His} mode of the G117I mutant of CooA was identified at 220 cm^{-1}, the same as that of Mb. Thus, Coyle et al. [35] proposed that the presence of a hydrogen bond between Asn42 and the proximal His (His77), as revealed in the X-ray structure of ferrous CooA,[25] strengthens the Fe−His bond of ferrous CooA. This is also observed in Mb, wherein Ser92 makes a weak hydrogen bond with the proximal His. However, considering that neither ν_{Fe-CO} nor ν_{C-O} are affected by the mutation of Asn42, it is likely that Asn42 does not form a hydrogen bond with His77 in the CO-bound form (the X-ray structure of CO-bound CooA is not yet available). Therefore, binding of CO to the ferrous CooA induces a conformational change on the proximal side of heme. This disrupts the interaction between Asn42 and His77, weakening the Fe−His bond of CooA, which results in the activation of CooA (part b of Figure 3).

A change in bond strength of the Fe−His bond upon CO binding also occurs in NPAS2. The electronegative character of the endogenous axial ligands can be deduced from the low frequency of the ν_{11} mode, especially in the ferrous state.[40,41] This band is known as a π-electron density marker and is related to the protonation state of the axial ligands. The ν_{11} frequency decreases with increasing donor strength of the axial ligands. The ν_{11} band of the ferrous PAS-A domain of NPAS2 was observed at 1533 cm^{-1}, which is 8 cm^{-1} lower than that of cytochrome c_3, in which the axial ligands are neutral histidines.[42] When Cys170 is replaced by Ala, this band was upshifted to 1539 cm^{-1}, implying that Cys170 is involved in a hydrogen-bonding network that directly or indirectly deprotonates the proximal His.[37] Because the presence of hydrogen bonding at the proximal His increases the anionic character of the imidazole ring and strengthens the Fe−His bond, the Fe−His bond of the ferrous PAS-A domain is stronger than that of cytochrome c_3. In contrast to the reduced PAS-A domain, the ν_{Fe-CO} and ν_{C-O} frequencies (Table 3)[37] fall on the line for hemoproteins with neutral His as a trans ligand (Figure 2), suggesting that the CO-bound form of the PAS-A domain has a neutral His as a trans ligand for CO. Therefore, CO binding weakens the Fe−His bond of the PAS-A domain, and this change would be transmitted to the dimerization interface with BMAL1.

Bovine lung sGC is a NO-sensing protein with a 5c-HS ferrous heme in the isolated state. This protein also utilizes the proximal pathways for transducing the ligand-binding signal (Figure 1). NO binds to the ferrous heme, increasing the guanylyl cyclase activity over a few 100-fold. This has been explained by the coordination structures of the NO-bound heme: when NO binds to sGC, the 6c-LS ferrous heme is generated first, but the Fe−His bond is subsequently broken to form a 5c NO−heme,[43,44] leading to a conformational change that increases the catalytic activity. In contrast to NO, CO can elevate the activity by only 4−5-fold.[45] When CO binds to heme, the Fe−His bond remains intact, forming an ordinary 6c CO−heme.[45,46] Therefore, the cleavage of the Fe−His bond is believed to be indispensable for activation of the enzyme.

Previously, an unusually low frequency of the Fe−His stretching mode of sGC (204 cm^{-1}) is thought to be correlated with the strong strain in the Fe−His bond.[47] Recently, proteins homologous to the heme-binding domain of sGC were found in bacteria through genomic analysis, and RR spectra were investigated.[48] VCA0720 and *Tt*Tar4H are cloned from *Vibrio cholerae* and *Thermoanaerobacter tengcongensis*, respectively. ν_{Fe-His} of VCA0720 and *Tt*Tar4H are 224 and 218 cm^{-1}, respectively, which

are higher than that of sGC. For addition of NO to the reduced form, VCA0720 gives a 5c-NO complex as sGC does, whereas *Tf*Tar4H forms a 6c-NO complex, although it has a smaller ν_{Fe-His} than that of VCA0720. These results suggest that the bond cleavage between iron and proximal His is not necessarily correlated with the ν_{Fe-His} frequency. Raman and co-workers solved the crystal structure of a homologous protein to the heme-binding domain of sGC from *Clostridium botulinum*.[49] It produces a stable 5c-NO complex, but the 5c-NO heme is converted to 6c-NO by replacement of Tyr139 with Phe, which is located in the distal side of the heme pocket and can contact with the iron-bound ligand, because of less steric crowding. Therefore, the structure of the distal side also plays a significant role in the modulation of the strength of the Fe−His bond.

Activation via Heme Peripheral Groups

As discussed above, there is a general consensus that CO is not a physiologically relevant activator of sGC. However, in the presence of an exogenous co-activator, such as 3-(5′-hydroxymethyl-2′-furyl)-1-benzylindazole (YC-1), CO can also activate the enzyme. Addition of YC-1 or CO alone activates sGC only 5-fold, whereas addition of both YC-1 and CO activates the enzyme to the same level as achieved by NO.[50] In the presence of YC-1, two Fe−CO stretching modes appear at 489 and 522 cm^{-1}.[51−53] Although the 489 cm^{-1} band comes from the 6c CO−heme, the 522 cm^{-1} band is derived from the 5c CO−heme. This seems to indicate that, as observed for NO-bound sGC, formation of a 5c heme causes the significant increase in the activity of sGC in the presence of YC-1 as observed for NO-bound sGC. Although it is difficult to estimate the population ratio of 5c and 6c CO−hemes by RR spectra, infrared spectroscopy shows the presence of a significant amount of 6c CO−sGC.[52] This suggests that the 5c species is minor; therefore, it alone cannot account for an activity comparable to that of NO−sGC. Thus, another activation mechanism besides formation of a 5c heme is likely to be involved in the synergistic activation of sGC by CO and YC-1.

Significant differences in the frequencies of the heme vinyl and propionate modes were observed in the absence and presence of YC-1. Addition of YC-1 and GTP to the CO-bound sGC shifted the vinyl bending mode from 424 to 400 cm^{-1} and changed the intensity ratio of the two vinyl stretching modes at 1600 and 1615 cm^{-1}.[53] Moreover, the intensity of the propionate bending mode, $\delta(C_\beta C_c C_d)$, at 396 cm^{-1} was significantly increased in the presence of YC-1 and GTP. These results suggest that the binding site of YC-1 is so close to the heme group that it can directly interact with vinyl and propionate groups of heme. A similar change was observed by addition of another allosteric effector, BAY-41-2272, to the CO-bound sGC.[54] In the crystal structures of the sGC-like heme domain from *T. tengcongensis* (*Tf*Tar4H), which has two slightly different structures, distorted and relaxed, in the different crystal packing, Arg135 makes strong hydrogen bonds with both

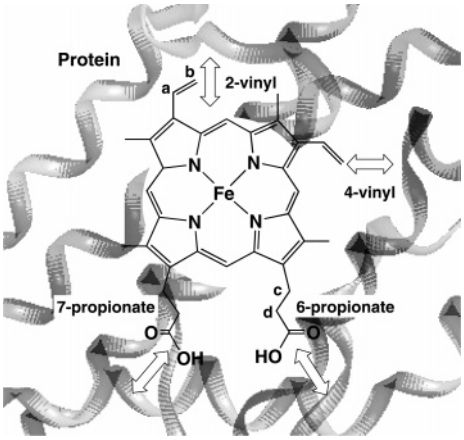

FIGURE 4. Structure of heme (protoporphyrin IX). White arrows represent the plausible interactions between heme side chains and surrounding amino acid residues.

propionate groups in the distorted form, whereas one of hydrogen bonds is cleaved in the relaxed form because of the movement of Arg135 induced by disruption of the interaction of Asp45.[55] Although there is no direct evidence at this moment, these results suggest that the heme peripheral groups could mediate transduction of the signal by sGC in the presence of YC-1. The heme peripheral groups, which would be involved in the signaling discussed here, are illustrated in Figure 4.

The propionate bending modes, $\delta(C_\beta C_c C_d)$, of the reduced and CO-bound *Ec* DOS are observed at 376 and 380 cm^{-1}, respectively.[56] The frequency of $\delta(C_\beta C_c C_d)$ is indicative of hydrogen bonding between the heme-7-propionate group and the surrounding amino acid residues.[57] In Mb, the heme-7-propionate group makes a hydrogen bond with His97 and Ser92, and the $\delta(C_\beta C_c C_d)$ mode appears at 376 cm^{-1}. The disruption of this hydrogen bond by His97 → Phe or His97 → Phe/Ser92 → Ala mutations leads to downshifts of the band by 10 and 11 cm^{-1}, respectively.[58] Recently, the X-ray crystallographic structures of the O_2-bound and unbound (reduced) *Ec* DOS were resolved.[17] In the O_2-bound form, the 7-propionate makes a strong hydrogen bond with Arg97, whereas, in the reduced form, it makes weak hydrogen bonds with the backbone NH of Met95 and two water molecules. This observation is compatible with the higher frequencies of the $\delta(C_\beta C_c C_d)$ mode in the O_2-bound form. After photolysis, no new prominent bands were observed in the 250−450 cm^{-1} region in the picosecond time scale of the time-resolved RR spectra for *Ec* DOS (unpublished data). This indicates that the heme peripheral modes of the photoproduct are identical to those of the CO-bound form. After a 20 ns delay, however, a weak $\delta(C_\beta C_c C_d)$ band appeared at 363 cm^{-1}. Because the lower $\delta(C_\beta C_c C_d)$ frequency accounts for a weak (or no) heme-7-propionate hydrogen bond, as discussed above, the hydrogen bond between 7-propionate and Arg97 must be cleaved within 20 ns of photolysis. Identical to observations in the reduced *Ec* DOS, this band was upshifted to 377 cm^{-1} 5 μs after photolysis, indicating the formation of a hydrogen bond. Accordingly, the shifts of the $\delta(C_\beta C_c C_d)$ mode during CO rebinding respond to the rearrangement of hydrogen

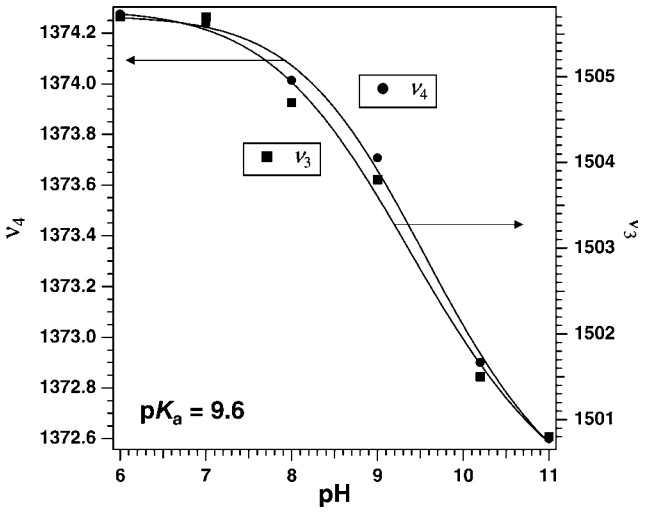

FIGURE 5. pH dependence of the frequencies of ν_4 (left axis) and ν_3 (right axis) modes of the ferric PAS-A domain of NPAS2.

bonds between 7-propionate and the surrounding amino acids and/or water molecules, which would lead to the conformational change related to the increase in catalytic activity. In the case of NPAS2, such a frequency shift during CO rebinding was not observed, suggesting that the process of transducing the ligand-binding signal does not include rearrangement of the hydrogen-bonding network.[37]

Redox- and pH-Dependent Ligand Switching

In some heme sensor proteins, an axial ligand of heme is replaced in a redox-dependent manner. For example, Cys75 of CooA, which is one of axial ligands in the ferric state, is replaced by His77 upon reduction of heme.[59] In *Ec* DOS, a water molecule is coordinated to the heme in the ferric form and displaced by Met95 upon reduction of heme.[18] Furthermore, for the PAS-A domain of NPAS2, Cys170 is the proximal ligand of heme in the ferric form, whereas His171 replaces it in the ferrous form.[37] Figure 5 shows the pH dependence of frequencies of the oxidation (ν_4) and spin-state marker (ν_3) bands of the ferric PAS-A domain of NPAS2. The ν_4 frequency of the PAS-A domain decreases by approximately 2 cm^{-1} as the pH increases, although this change is within the characteristic frequency region of ferric hemes. The frequency of ν_4 reflects the electron density in the porphyrin π^* orbital,[21,60] which is mixed with the iron d_π orbital. Because the d_π electrons are pushed out when σ donation from the axial ligand becomes larger, the electron density in the porphyrin π^* orbital increases. As a result, the ν_4 frequency decreases as the σ-electron donation increases.[40,61] Thus, the pH-dependent frequency shift of the ν_4 band shown in Figure 5 suggests a stronger σ-donor character from the axial ligand at higher pH. The ν_3 band is also downshifted from 1506 to 1501 cm^{-1} as the pH increases from 6 to 11, and the pH dependence is almost the same as that of the ν_4 band (Figure 5). These results may indicate that Cys170 is replaced by His at lower pH, while the 6c-LS state is retained. The pK_a value of 9.6 supports the involvement of cysteine in this reaction. Thus, as illustrated in Figure

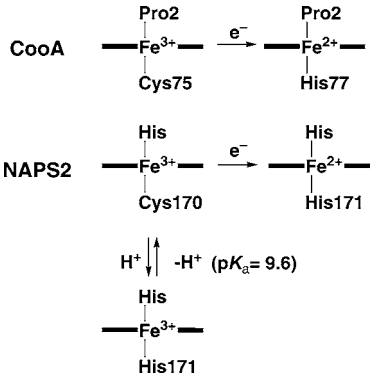

FIGURE 6. Coordination structures of the heme in CooA and the PAS-A domain of NPAS2.

6, the heme environment of these sensor proteins appears to be flexible enough to be rearranged by the redox and pH changes. This structural flexibility might be one of the characteristic features of the heme-based sensory proteins.

Ligand Discrimination between O_2 and CO

Upon NO or CO binding, sGC increases the catalytic activity of the conversion of GTP to cGMP. However, the presence of O_2 has a minimal effect on the enzymatic activity of sGC because of the extremely low affinity for O_2,[62] even though O_2 generally binds easily to a ferrous 5c heme in a protein. The frequencies of ν_{Fe-CO} and ν_{C-O} (Table 3) suggest that the low O_2 affinity is due to the negative polarity in its distal pocket. The ν_{Fe-CO} of CO-bound sGC appears at 473 cm^{-1},[47,63] which is one of the lowest ν_{Fe-CO} frequencies among the known heme proteins. In the case of Mb, introduction of a negative charge by the Val68 → Thr mutation and removal of a positive charge by the replacement of distal His with Val (H64V/V68T double mutant) causes a low-frequency shift in the ν_{Fe-CO} mode from 509 to 477 cm^{-1}.[32] Therefore, the very low frequency of ν_{Fe-CO} can indicate the negativity of the heme pocket of sGC.

Furthermore, the negative polarity of the heme pocket of sGC is reflected in its kinetics. The correlation between the electrostatic field of the distal heme pocket and the dissociation rate constants of O_2, CO, and NO was examined by Phillips and co-workers.[30] They concluded that the O_2 dissociation rate strongly depends on the electrostatic field at the ligand-binding site, whereas CO and NO dissociation rates are weakly dependent and essentially not dependent on it, respectively. This is due to the highly polar Fe−O_2 bond, which is nearly as polar as an Fe^{3+}−O_2^- bond and is stabilized by the positive field of the distal histidine in Hb and Mb. Accordingly, the negative heme pocket of sGC can reduce the affinity of O_2 so that it can discriminate between the effector molecules, namely, NO and CO.

HemAT can also distinguish O_2 from other diatomic gaseous molecules. Close inspection of the RR spectrum of O_2-bound HemAT reveals that the low-frequency region of the spectrum is composed of three oxygen isotope-sensitive bands at 554, 566, and 572 cm^{-1}, which are assigned to the closed, open α, and open β forms,

respectively.[64] This is the first observation of multiple conformations of the heme−O_2 complex. The ν_{Fe-O_2} frequency of the closed form at 554 cm^{-1} is approximately 15 cm^{-1} lower than that observed for mammalian Hb and Mb,[65] and it is the lowest ν_{Fe-O_2} frequency among the known hemoproteins. Yeh et al. proposed that hydrogen bonding to both the proximal (directly bonded to iron) and the terminal oxygen atoms of the heme-bound O_2 results in the significant lowering of the ν_{Fe-O_2} frequency.[66,67] Therefore, the noticeably low frequency of the ν_{Fe-O_2} mode of HemAT suggests the presence of strong hydrogen bonding to the iron-bound O_2. The disappearance of the 554 cm^{-1} band in the Thr95 → Ala mutant supports the idea that Thr95 forms a strong hydrogen bond to the iron-bound O_2, which is characteristic of O_2-bound HemAT in the closed form.

On the basis of the correlation plot between ν_{Fe-CO} and ν_{C-O} (Figure 2), the positive polarity near the bound ligand through such hydrogen bonding is expected to yield a higher ν_{Fe-CO} frequency. In fact, Hb from *Mycobacterium tuberculosis* has lower ν_{Fe-O_2} (560 cm^{-1}) and higher ν_{Fe-CO} (535 cm^{-1}) frequencies.[66] Unexpectedly, however, ν_{Fe-CO} of HemAT was observed at 494 cm^{-1} (Table 3),[68] which is comparable to the frequencies for the Mb mutants in which the distal histidine was replaced by a nonpolar residue (H64L in Figure 2). This means that the CO-bound HemAT has a less polar heme pocket, which is in contrast to the highly polar heme pocket of the O_2-bound form.

The ν_{Fe-O_2} frequency of *Ec* DOS (561 cm^{-1}) is also low. In agreement with these Raman results, recent X-ray crystal structures of O_2-bound *Ec* DOS indicate that Arg97 forms a hydrogen bond with bound O_2.[17] However, the ν_{Fe-CO} of CO-bound *Ec* DOS is again low (486 cm^{-1}), suggesting that the mechanism for discriminating ligands in HemAT is the same as that in *Ec* DOS.[56] Presumably, rearrangements of hydrogen bonds around the heme distal pocket, which could take place upon ligand binding, discriminate the effector molecule from other diatomic molecules.

Concluding Remarks

Heme-based sensor proteins are a newly discovered class of hemoproteins in which the functional activities are regulated by heme ligand binding. In this Account, we have used the currently available RR spectroscopic studies to characterize the mechanism by which the heme-containing sensor domain detects target molecules. The RR spectra have revealed the conformational changes at the heme distal and proximal sites as well as the heme peripheral (propionate and vinyl) modes associated with ligand binding. These studies identified significant conformational changes that occur during ligand binding, including outward movement of the endogenous axial ligand from the heme pocket and cleavage of the trans Fe−ligand (endogenous) bond upon binding of an exogenous ligand to the axial position of iron. In addition, these studies revealed slight conformational changes that occur upon ligand binding, including modulation of the bond strength of the Fe−His bond and cleavage of the hydrogen bond between the heme peripheral groups and the surrounding amino acids. However, although we discussed here three different signal transduction pathways separately for convenience, these mechanisms are not always independent events. For example, deprotonation of distal His is communicated with that of proximal His as shown in horseradish peroxide (HRP).[69] The real image of signal transduction would be mixed with these (or more) mechanisms.

We thank our collaborators, Professors Toru Shimizu and Ikuko Sagami, for the work on NPAS2 and Prof. Shigetoshi Aono for the work on CooA and HemAT. This work was supported by Grants-in-Aid from the Ministry of Education, Culture, Sports, Science, and Technology, Japan to T. K. (14001004).

References

(1) Scott, R. A.; Mauk, A. G. *Cytochrome c—A Multidisciplinary Approach*; University Science Books: Sausalito, CA, 1996.
(2) Gray, H. B.; Winkler, J. R. Electron transfer in proteins. *Annu. Rev. Biochem.* **1996**, *65*, 537−561.
(3) Antonini, E.; Brunori, M. *Hemoglobin and Myoglobin in Their Reactions with Ligands*; North-Holland Publishing Co.: Amsterdam, The Netherlands, 1971.
(4) Ortiz de Montellano, P. R. *Cytochrome P450: Structure, Mechanism, and Biochemistry*; Plenum Press: New York, 1995.
(5) Dunford, H. B. *Heme peroxidases*; John Wiley: New York, 1999.
(6) Rodgers, K. R. Heme-based sensors in biological systems. *Curr. Opin. Chem. Biol.* **1999**, *3*, 158−167.
(7) Chan, M. K. Recent advances in heme-protein sensors. *Curr. Opin. Chem. Biol.* **2001**, *5*, 216−222.
(8) Aono, S. Biochemical and biophysical properties of the CO-sensing transcriptional activator CooA. *Acc. Chem. Res.* **2003**, *36*, 825−831.
(9) Nagai, M.; Wajcman, H.; Lahary, A.; Nakatsukasa, T.; Nagatomo, S.; Kitagawa, T. Quaternary structure sensitive tyrosine residues in human hemoglobin: UV resonance Raman studies of mutants at α140, β35, and β145 tyrosine. *Biochemistry* **1999**, *38*, 1243−1251.
(10) Balakrishnan, G.; Tsai, C. H.; Wu, Q.; Case, M. A.; Pevsner, A.; McLendon, G. L.; Ho, C.; Spiro, T. G. Hemoglobin site-mutants reveal dynamical role of interhelical H-bonds in the allosteric pathway: Time-resolved UV resonance Raman evidence for intradimer coupling. *J. Mol. Biol.* **2004**, *340*, 857−868.
(11) Friebe, A.; Koesling, D. Regulation of nitric oxide-sensitive guanylyl cyclase. *Circ. Res.* **2003**, *93*, 96−105.
(12) Wedel, B.; Humbert, P.; Harteneck, C.; Foerster, J.; Malkewitz, J.; Bohme, E.; Schultz, G.; Koesling, D. Mutation of His-105 in the β_1 subunit yields a nitric oxide-insensitive form of soluble guanylyl cyclase. *Proc. Natl. Acad. Sci. U.S.A.* **1994**, *91*, 2592−2596.
(13) Zhao, Y.; Schelvis, J. P. M.; Babcock, G. T.; Marletta, M. A. Identification of histidine 105 in the β1 subunit of soluble guanylate cyclase as the heme proximal ligand. *Biochemistry* **1998**, *37*, 4502−4509.
(14) Gilles-Gonzalez, M. A.; Ditta, G. S.; Helinski, D. R. A haemoprotein with kinase activity encoded by the oxygen sensor of *Rhizobium meliloti*. *Nature* **1991**, *350*, 170−172.
(15) Sasakura, Y.; Hirata, S.; Sugiyama, S.; Suzuki, S.; Taguchi, S.; Watanabe, M.; Matsui, T.; Sagami, I.; Shimizu, T. Characterization of a direct oxygen sensor heme protein from *Escherichia coli*. Effects of the heme redox states and mutations at the heme-binding site on catalysis and structure. *J. Biol. Chem.* **2002**, *277*, 23821−23827.
(16) Gong, W.; Hao, B.; Chan, M. K. New mechanistic insights from structural studies of the oxygen-sensing domain of *Bradyrhizobium japonicum* FixL. *Biochemistry* **2000**, *39*, 3955−3962.
(17) Park, H.; Suquet, C.; Satterlee, J. D.; Kang, C. Insights into signal transduction involving PAS domain oxygen-sensing heme proteins from the X-ray crystal structure of *Escherichia coli* Dos heme domain (*Ec* DosH). *Biochemistry* **2004**, *43*, 2738−2746.
(18) Kurokawa, H.; Lee, D. S.; Watanabe, M.; Sagami, I.; Mikami, B.; Raman, C. S.; Shimizu, T. A redox-controlled molecular switch revealed by the crystal structure of a bacterial heme PAS sensor. *J. Biol. Chem.* **2004**, *279*, 20186−20193.
(19) Roberts, G. P.; Youn, H.; Kerby, R. L. CO-sensing mechanisms. *Microbiol. Mol. Biol. Rev.* **2004**, *68*, 453−473.

(20) Taoka, S.; Banerjee, R. Characterization of NO binding to human cystathionine β-synthase: Possible implications of the effects of CO and NO binding to the human enzyme. *J. Inorg. Biochem.* **2001**, *87*, 245−251.
(21) Spiro, T. G.; Li, X.-Y. Resonance Raman spectroscopy of metalloporphyrin. In *Biological Applications of Raman Spectroscopy*; Spiro, T. G., Ed.; John Wiley and Sons: New York, 1988; Vol. 3, pp 1−37.
(22) Abe, M.; Kitagawa, T.; Kyogoku, Y. Resonance Raman-spectra of octaethylporphyrinato-Ni^{II} and meso-deuterated and ^{15}N-substituted derivatives. II. A normal coordinate analysis. *J. Chem. Phys.* **1978**, *69*, 4526−4534.
(23) Wells, A. V.; Li, P.; Champion, P. M.; Martinis, S. A.; Sligar, S. G. Resonance Raman investigations of *Escherichia coli*-expressed *Pseudomonas putida* cytochrome P450 and P420. *Biochemistry* **1992**, *31*, 4384−4393.
(24) Shelver, D.; Kerby, R. L.; He, Y. P.; Roberts, G. P. CooA, a CO-sensing transcription factor from *Rhodospirillum rubrum*, is a CO-binding heme protein. *Proc. Natl. Acad. Sci. U.S.A.* **1997**, *94*, 11216−11220.
(25) Lanzilotta, W. N.; Schuller, D. J.; Thorsteinsson, M. V.; Kerby, R. L.; Roberts, G. P.; Poulos, T. L. Structure of the CO sensing transcription activator CooA. *Nat. Struct. Biol.* **2000**, *7*, 876−880.
(26) Uchida, T.; Ishikawa, H.; Ishimori, K.; Morishima, I.; Nakajima, H.; Aono, S.; Mizutani, Y.; Kitagawa, T. Identification of histidine 77 as the axial heme ligand of carbonmonoxy CooA by picosecond time-resolved resonance Raman spectroscopy. *Biochemistry* **2000**, *39*, 12747−12752.
(27) Yamamoto, K.; Ishikawa, H.; Takahashi, S.; Ishimori, K.; Morishima, I.; Nakajima, H.; Aono, S. Binding of CO at the Pro2 side is crucial for the activation of CO-sensing transcriptional activator CooA. ^{1}H NMR spectroscopic studies. *J. Biol. Chem.* **2001**, *276*, 11473−11476.
(28) Ray, G. B.; Li, X. Y.; Ibers, J. A.; Sessler, J. L.; Spiro, T. G. How far can proteins bend the FeCO unit—Distal polar and steric effects in heme-proteins and models. *J. Am. Chem. Soc.* **1994**, *116*, 162−176.
(29) Li, T. S.; Quillin, M. L.; Phillips, G. N.; Olson, J. S. Structural determinants of the stretching frequency of CO bound to myoglobin. *Biochemistry* **1994**, *33*, 1433−1446.
(30) Phillips, G. N., Jr; Teodoro, M. L.; Li, T. S.; Smith, B.; Olson, J. S. Bound CO is a molecular probe of electrostatic potential in the distal pocket of myoglobin. *J. Phys. Chem. B* **1999**, *103*, 8817−8829.
(31) Ling, J.; Li, T.; Olson, J. S.; Bocian, D. F. Identification of the iron−carbonyl stretch in distal histidine mutants of carbonmonoxymyoglobin. *Biochim. Biophys. Acta* **1994**, *1188*, 417−421.
(32) Anderton, C. L.; Hester, R. E.; Moore, J. N. A chemometric analysis of the resonance Raman spectra of mutant carbonmonoxymyoglobins reveals the effects of polarity. *Biochim. Biophys. Acta* **1997**, *1338*, 107−120.
(33) Uchida, T.; Ishikawa, H.; Takahashi, S.; Ishimori, K.; Morishima, I.; Ohkubo, K.; Nakajima, H.; Aono, S. Heme environmental structure of CooA is modulated by the target DNA binding. Evidence from resonance Raman spectroscopy and CO rebinding kinetics. *J. Biol. Chem.* **1998**, *273*, 19988−19992.
(34) Vogel, K. M.; Spiro, T. G.; Shelver, D.; Thorsteinsson, M. V.; Roberts, G. P. Resonance Raman evidence for a novel charge relay activation mechanism of the CO-dependent heme protein transcription factor CooA. *Biochemistry* **1999**, *38*, 2679−2687.
(35) Coyle, C. M.; Puranik, M.; Youn, H.; Nielsen, S. B.; Williams, R. D.; Kerby, R. L.; Roberts, G. P.; Spiro, T. G. Activation mechanism of the CO sensor CooA. Mutational and resonance Raman spectroscopic studies. *J. Biol. Chem.* **2003**, *278*, 35384−35393.
(36) Dioum, E. M.; Rutter, J.; Tuckerman, J. R.; Gonzalez, G.; Gilles-Gonzalez, M. A.; McKnight, S. L. NPAS2: A gas-responsive transcription factor. *Science* **2002**, *298*, 2385−2387.
(37) Uchida, T.; Sato, E.; Sato, A.; Sagami, I.; Shimizu, T.; Kitagawa, T. CO-dependent activity-controlling mechanism of heme-containing CO-sensor protein, neuronal PAS domain protein 2. *J. Biol. Chem.* **2005**, *280*, 21358−21368.
(38) Mukai, M.; Nakamura, K.; Nakamura, H.; Iizuka, T.; Shiro, Y. Roles of Ile209 and Ile210 on the heme pocket structure and regulation of histidine kinase activity of oxygen sensor FixL from *Rhizobium meliloti*. *Biochemistry* **2000**, *39*, 13810−13816.
(39) Yeh, S. R. A novel intersubunit communication mechanism in a truncated hemoglobin from *Mycobacterium tuberculosis*. *J. Phys. Chem. B* **2004**, *108*, 1478−1484.
(40) Desbois, A.; Lutz, M. Redox control of proton transfers in membrane *b*-type cytochromes—An absorption and resonance Raman study on bis(imidazole) and bis(imidazolate) model complexes of iron-protoporphyrin. *Eur. Biophys. J.* **1992**, *20*, 321−335.
(41) Othman, S.; Le Lirzin, A.; Desbois, A. Resonance Raman investigation of imidazole and imidazolate complexes of microperoxidase: Characterization of the bis(histidine) axial ligation in *c*-type cytochromes. *Biochemistry* **1994**, *33*, 15437−15448.
(42) Verma, A. L.; Kimura, K.; Nakamura, A.; Yagi, T.; Inokuchi, H.; Kitagawa, T. Resonance Raman studies of hydrogenase-catalyzed reduction of cytochrome c_3 by hydrogen. Evidence for heme−heme interactions. *J. Am. Chem. Soc.* **1988**, *110*, 6617−6623.
(43) Lawson, D. M.; Stevenson, C. E.; Andrew, C. R.; George, S. J.; Eady, R. R. A two-faced molecule offers NO explanation: The proximal binding of nitric oxide to haem. *Biochem. Soc. Trans.* **2003**, *31*, 553−557.
(44) Russwurm, M.; Koesling, D. NO activation of guanylyl cyclase. *EMBO J.* **2004**, *23*, 4443−4450.
(45) Stone, J. R.; Marletta, M. A. Soluble guanylate cyclase from bovine lung: Activation with nitric oxide and carbon monoxide and spectral characterization of the ferrous and ferric states. *Biochemistry* **1994**, *33*, 5636−5640.
(46) Yu, A. E.; Hu, S. Z.; Spiro, T. G.; Burstyn, J. N. Resonance Raman spectroscopy of soluble guanylyl cyclase reveals displacement of distal and proximal heme ligands by NO. *J. Am. Chem.* Soc. **1994**, *116*, 4117−4118.
(47) Deinum, G.; Stone, J. R.; Babcock, G. T.; Marletta, M. A. Binding of nitric oxide and carbon monoxide to soluble guanylate cyclase as observed with resonance Raman spectroscopy. *Biochemistry* **1996**, *35*, 1540−1547.
(48) Karow, D. S.; Pan, D.; Tran, R.; Pellicena, P.; Presley, A.; Mathies, R. A.; Marletta, M. A. Spectroscopic characterization of the soluble guanylate cyclase-like heme domains from *Vibrio cholerae* and *Thermoanaerobacter tengcongensis*. *Biochemistry* **2004**, *43*, 10203−10211.
(49) Nioche, P.; Berka, V.; Vipond, J.; Minton, N.; Tsai, A. L.; Raman, C. S. Femtomolar sensitivity of a NO sensor from *Clostridium botulinum*. *Science* **2004**, *306*, 1550−1553.
(50) Stone, J. R.; Marletta, M. A. Synergistic activation of soluble guanylate cyclase by YC-1 and carbon monoxide: Implications for the role of cleavage of the iron−histidine bond during activation by nitric oxide. *Chem. Biol.* **1998**, *5*, 255−261.
(51) Denninger, J. W.; Schelvis, J. P.; Brandish, P. E.; Zhao, Y.; Babcock, G. T.; Marletta, M. A. Interaction of soluble guanylate cyclase with YC-1: Kinetic and resonance Raman studies. *Biochemistry* **2000**, *39*, 4191−4198.
(52) Makino, R.; Obayashi, E.; Homma, N.; Shiro, Y.; Hori, H. YC-1 facilitates release of the proximal His residue in the NO and CO complexes of soluble guanylate cyclase. *J. Biol. Chem.* **2003**, *278*, 11130−11137.
(53) Pal, B.; Kitagawa, T. Interactions of soluble guanylate cyclase with diatomics as probed by resonance Raman spectroscopy. *J. Inorg. Biochem.* **2005**, *99*, 267−279.
(54) Martin, E.; Czarneck, K.; Jayaraman, V.; Murad, F.; Kincaid, J. Resonance Raman and infrared spectroscopic studies of high-output forms of human soluble guanylyl cyclase. *J. Am. Chem. Soc.* **2005**, *127*, 4625−4631.
(55) Pellicena, P.; Karow, D. S.; Boon, E. M.; Marletta, M. A.; Kuriyan, J. Crystal structure of an oxygen-binding heme domain related to soluble guanylate cyclases. *Proc. Natl. Acad. Sci. U.S.A.* **2004**, *101*, 12854−12859.
(56) Sato, A.; Sasakura, Y.; Sugiyama, S.; Sagami, I.; Shimizu, T.; Mizutani, Y.; Kitagawa, T. Stationary and time-resolved resonance Raman spectra of His77 and Met95 mutants of the isolated heme domain of a direct oxygen sensor from *Escherichia coli*. *J. Biol. Chem.* **2002**, *277*, 32650−32658.
(57) Cerda-Colon, J. F.; Silfa, E.; Lopez-Garriga, J. Unusual rocking freedom of the heme in the hydrogen sulfide-binding hemoglobin from *Lucina pectinata*. *J. Am. Chem. Soc.* **1998**, *120*, 9312−9317.
(58) Peterson, E. S.; Friedman, J. M.; Chien, E. Y.; Sligar, S. G. Functional implications of the proximal hydrogen-bonding network in myoglobin: A resonance Raman and kinetic study of Leu89, Ser92, His97, and F-helix swap mutants. *Biochemistry* **1998**, *37*, 12301−12319.
(59) Aono, S.; Ohkubo, K.; Matsuo, T.; Nakajima, H. Redox-controlled ligand exchange of the heme in the CO-sensing transcriptional activator CooA. *J. Biol. Chem.* **1998**, *273*, 25757−25764.
(60) Kitagawa, T.; Kyogoku, Y.; Iizuka, T.; Ikeda-Saito, M. Nature of the iron−ligand bond in ferrous low spin hemoproteins studied by resonance Raman scattering. *J. Am. Chem. Soc.* **1976**, *98*, 5169−5173.
(61) Anzenbacher, P.; Evangelistakirkup, R.; Schenkman, J.; Spiro, T. G. Influence of thiolate ligation on the heme electronic-structure in microsomal cytochrome-P-450 and model compounds—Resonance Raman spectroscopic evidence. *Inorg. Chem.* **1989**, *28*, 4491−4495.

(62) Gerzer, R.; Bohme, E.; Hofmann, F.; Schultz, G. Soluble guanylate cyclase purified from bovine lung contains heme and copper. *FEBS Lett.* **1981**, *132*, 71−74.
(63) Kim, S. Y.; Deinum, G.; Gardner, M. T.; Marletta, M. A.; Babcock, G. T. Distal pocket polarity in the unusual ligand binding site of soluble guanylate cyclase: Implications for the control of ·NO binding. *J. Am. Chem. Soc.* **1996**, *118*, 8769−8770.
(64) Ohta, T.; Yoshimura, H.; Yoshioka, S.; Aono, S.; Kitagawa, T. Oxygen-sensing mechanism of HemAT from *Bacillus subtilis*: A resonance Raman spectroscopic study. *J. Am. Chem. Soc.* **2004**, *126*, 15000−15001.
(65) Hirota, S.; Li, T. S.; Phillips, G. N., Jr.; Olson, J. S.; Mukai, M.; Kitagawa, T. Perturbation of the $Fe-O_2$ bond by nearby residues in heme pocket: Observation of ν_{Fe-O_2} Raman bands for oxymyoglobin mutants. *J. Am. Chem. Soc.* **1996**, *118*, 7845−7846.
(66) Yeh, S. R.; Couture, M.; Ouellet, Y.; Guertin, M.; Rousseau, D. L. A cooperative oxygen binding hemoglobin from *Mycobacterium tuberculosis*. Stabilization of heme ligands by a distal tyrosine residue. *J. Biol. Chem.* **2000**, *275*, 1679−1684.
(67) Das, T. K.; Friedman, J. M.; Kloek, A. P.; Goldberg, D. E.; Rousseau, D. L. Origin of the anomalous Fe−CO stretching mode in the CO complex of *Ascaris* hemoglobin. *Biochemistry* **2000**, *39*, 837−842.
(68) Aono, S.; Kato, T.; Matsuki, M.; Nakajima, H.; Ohta, T.; Uchida, T.; Kitagawa, T. Resonance Raman and ligand binding studies of the oxygen-sensing signal transducer protein HemAT from *Bacillus subtilis*. *J. Biol. Chem.* **2002**, *277*, 13528−13538.
(69) Teraoka, J.; Kitagawa, T. Structural implication of the heme-linked ionization of horseradish peroxidase probed by the Fe-histidine stretching Raman line. *J. Biol. Chem.* **1981**, *256*, 3969−3977.
(70) Fan, B.; Wang, J.; Stuehr, D. J.; Rousseau, D. L. NO synthase isozymes have distinct substrate binding sites. *Biochemistry* **1997**, *36*, 12660−12665.
(71) Rodgers, K. R.; Lukat-Rodgers, G. S.; Barron, J. A. Structural basis for ligand discrimination and response initiation in the heme-based oxygen sensor FixL. *Biochemistry* **1996**, *35*, 9539−9548.
(72) Tamura, K.; Nakamura, H.; Tanaka, Y.; Oue, S.; Tsukamoto, K.; Nomura, M.; Tsuchiya, T.; Adachi, S.; Takahashi, S.; Iizuka, T.; Shiro, Y. Nature of endogenous ligand binding to heme iron in oxygen sensor FixL. *J. Am. Chem. Soc.* **1996**, *118*, 9434−9435.
(73) Lukat-Rodgers, G. S.; Rodgers, K. R. Characterization of ferrous FixL-nitric oxide adducts by resonance Raman spectroscopy. *Biochemistry* **1997**, *36*, 4178−4187.

AR030267D